

Dipole interaction and magnetic anisotropy in gadolinium compounds

M. Rotter*

*Institut für Physikalische Chemie, Universität Wien, A-1090 Wien, Austria
and Institut für Festkörperphysik, Technische Universität Dresden, D-01062 Dresden, Germany*

M. Loewenhaupt and M. Doerr

Institut für Festkörperphysik, Technische Universität Dresden, D-01062 Dresden, Germany

A. Lindbaum and H. Sassik

Institut für Festkörperphysik, Technische Universität Wien, Wiedner Hauptstraße 8-10, A-1040 Wien, Austria

K. Ziebeck

Department of Physics, Loughborough University, Loughborough, LE 11 3TK, United Kingdom

B. Beuneu

Laboratoire Léon Brillouin, CEA-CNRS, Saclay, 91191 Gif sur Yvette Cedex, France

(Received 2 June 2003; published 15 October 2003)

The influence of the dipole interaction on the magnetic anisotropy of Gd compounds is investigated. Available data on ferromagnets and antiferromagnets with different crystal structures are discussed and complemented by new neutron scattering experiments on GdCu_2In , GdAu_2Si_2 , GdAu_2 , and GdAg_2 . If the propagation vector of the magnetic structure is known, the orientation of the magnetic moments as caused by the dipole interaction can be predicted by a straightforward numerical method for compounds with a single Gd atom in the primitive unit cell. The moment directions found by magnetic diffraction on GdAu_2Si_2 , GdAu_2 , GdAg_2 , GdCu_2Si_2 , $\text{GdNi}_2\text{B}_2\text{C}$, GdNi_2Si_2 , $\text{GdBa}_2\text{Cu}_3\text{O}_7$, GdNi_5 , GdCuSn , GdCu_2In , GdCu_4In , and GdX ($X = \text{Ag}, \text{Cu}, \text{S}, \text{Se}, \text{Sb}, \text{As}, \text{Bi}, \text{P}$) are compared to the predicted directions resulting in an almost complete accordance. Therefore, the dipole interaction is identified as the dominating source of anisotropy for most Gd compounds. The numerical method can be applied to a large number of other compounds with zero angular momentum.

DOI: 10.1103/PhysRevB.68.144418

PACS number(s): 75.30.Gw, 75.50.Ee, 75.25.+z

I. INTRODUCTION

The sources of magnetic anisotropy of rare earth compounds are single ion, dipolar, and exchange anisotropy. The largest contribution usually comes from single ion anisotropy, unless the angular momentum is zero ($L=0$) such as in the case of Gd^{3+} . The exchange anisotropy may be large for $L \neq 0$ due to the spin-orbit interaction.¹ The small but finite magnetic anisotropy of $L=0$ rare earth compounds is topic of various speculations about its origin: An important contribution can come from the dipole interaction.² Also crystal field and exchange effects coming from higher multiplets have been discussed as the source.^{3,4} Recently, the role of biquadratic exchange for the magnetic properties of these ($L=0$) compounds has been pointed out.⁵ Different methods for the study of the anisotropy of the exchange interaction (i.e., the determination of the exchange tensor) have been suggested.⁶ This is still an experimental challenge for neutron scattering but only few quantitative results have been reported.⁷⁻¹⁰

It is well accepted, that the dipole interaction drives the anisotropy of Gd metal.^{2,11-14} Its influence leads to a modification of the critical dynamics, and the corresponding universality class has been identified.^{15,16} Recent first principles calculations¹⁷ indicate an equally large contribution arising from the spin orbit coupling of the conduction bands.

In Gd compounds few investigations of the anisotropy of

magnetic interactions have been performed and no systematic study is available, especially on antiferromagnets. Recently the ferromagnet GdNi_5 has been analyzed by muon spin resonance.¹⁸ In the past electron paramagnetic resonance in some Gd systems diluted with La or Y has been used to determine the exchange anisotropy between Gd ions.¹⁹ $\text{GdBa}_2\text{Cu}_3\text{O}_7$ has been diluted by Y and electron spin resonance spectra support the dominance of the dipolar anisotropy in this compound.³

In this paper we present a systematic study of Gd compounds with one Gd atom in the primitive unit cell. In these compounds the direction of the magnetic moments can be predicted from the knowledge of the propagation vector. We will show that it is possible to draw conclusions about the dominant interaction driving the magnetic anisotropy.

II. DIPOLAR MODEL

If the propagation vector $\boldsymbol{\tau}$ of a magnetic compound has been determined from neutron or magnetic x-ray diffraction data, it is possible to calculate that orientation of the magnetic moments in the ordered state, that is favored by the dipole interaction. For a detailed description of the analytical method, which is strictly valid near the ordering temperature, we refer to Ref. 20. Here we outline only the main steps of the calculation:

A general two ion coupling which depends only on the

dipolar moments of the 4*f* electrons is

$$\mathcal{H} = -\frac{1}{2} \sum_{ij} J_i^\alpha \mathcal{J}_{\alpha\beta}(ij) J_j^\beta. \quad (1)$$

In expression (1) the 4*f* moment of the *i*th Gd³⁺ ion is represented by the three components of the angular momentum operator J_i^α ($\alpha=1,2,3$).

In order to calculate the orientation of the magnetic moments, it is necessary to calculate the Fourier transform $\mathcal{J}_{\alpha\beta}(\boldsymbol{\tau})$ of the interaction tensor $\mathcal{J}_{\alpha\beta}(ij)$:

$$\mathcal{J}_{\alpha\beta}(\boldsymbol{\tau}) = \sum_j \mathcal{J}_{\alpha\beta}(ij) e^{-i\boldsymbol{\tau}(\mathbf{R}_i - \mathbf{R}_j)}. \quad (2)$$

For the following calculations we used the dipole interaction as given by

$$\mathcal{J}_{\alpha\beta}(ij) = (g_J \mu_B)^2 \frac{3(R_i^\alpha - R_j^\alpha)(R_i^\beta - R_j^\beta) - \delta_{\alpha\beta} |\mathbf{R}_i - \mathbf{R}_j|^2}{|\mathbf{R}_i - \mathbf{R}_j|^5}. \quad (3)$$

Here \mathbf{R}_i denotes the lattice vector of the *i*th Gd ion, g_J the Landé factor and μ_B the Bohr magneton.

The sum in Eq. (2) is evaluated numerically neglecting the contributions for distances between Gd ions that are larger than a maximum distance R_{\max} . The next step is to diagonalize the Fourier transform $\mathcal{J}_{\alpha\beta}(\boldsymbol{\tau})$. The predicted moment direction is given by the eigenvector corresponding to the largest eigenvalue.

Note that any *isotropic* contribution to the exchange interaction (such as Heisenberg or RKKY type interactions) is usually much larger and therefore determines the ordering temperature but will not influence the *anisotropic* behavior including the orientation of the magnetic moments. It should also be mentioned, that if high accuracy for the components of the Fourier transform $\mathcal{J}_{\alpha\beta}(\boldsymbol{\tau})$ is needed, analytical methods have to be used for the calculation.¹¹ Because of the long range of the interaction, the numerical procedure may converge slowly. This is important in some special cases, when the propagation vector and the geometry of the lattice cause a very small anisotropy of the dipole interaction and other interactions or surface effects may influence the orientation of the magnetic moments.²¹

As an example, Fig. 1 illustrates the issue of convergence of the eigenvalues for the body centered tetragonal lattice of GdAu₂Si₂. For the calculation the propagation vector $\boldsymbol{\tau}=(1/2 \ 0 \ 1/2)$ has been used, which has been determined from the neutron diffraction experiment described in the following. Δ_1 and Δ_2 denote differences of eigenvalues, which are a measure of the dipolar anisotropy between the three orthogonal directions shown in Fig. 1. The largest eigenvalue of $\mathcal{J}_{\alpha\beta}(\boldsymbol{\tau})$ corresponds to the eigenvector [010]. Therefore, the calculation predicts that the magnetic moments are aligned along the [010] direction.

III. NEUTRON DIFFRACTION

In order to enlarge the available set of scattering data on Gd compounds we have collected data on some cubic and

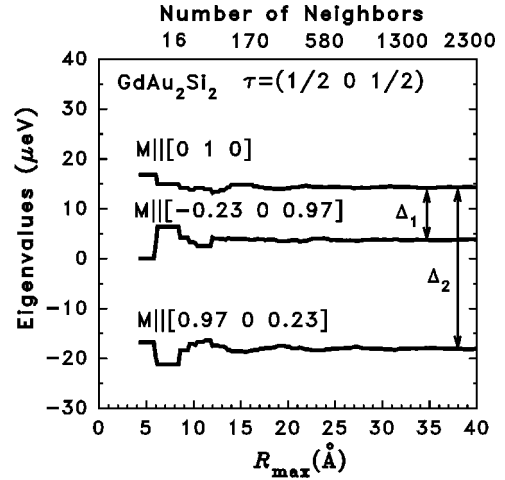


FIG. 1. Convergence behavior of the eigenvalues of $\mathcal{J}_{\alpha\beta}(\boldsymbol{\tau})$ of GdAu₂Si₂ with respect to the maximum distance R_{\max} of neighbors considered. The different lines correspond to eigenvectors representing moment directions parallel to $\mathbf{e}_0 = [0 \ 1 \ 0]$, $\mathbf{e}_1 = [-0.23 \ 0 \ 0.97]$, and $\mathbf{e}_2 = [0.97 \ 0 \ 0.23]$ (mind: in order to show that these vectors are orthonormal, the components are given with respect to euclidian coordinate system, not with respect to crystallographic lattice. The orientation is $x||a$, $y||b$ and $z||c$.) Δ_1 and Δ_2 indicate differences of eigenvalues, which are a measure of the dipolar anisotropy.

tetragonal Gd systems using the 7C2—hot source diffractometer of the Laboratoire Leon Brillouin (LLB), Saclay with a neutron wavelength of 0.58 Å. The absorption of the samples was reduced by using a double wall cylindrical sample holder (outer diameter 12 mm, inner diameter 10 mm). In the following we outline in detail the experimental results and show how they correspond to the predictions of the dipolar model.

A. GdAu₂Si₂

GdAu₂Si₂ orders antiferromagnetically at $T_N = 12$ K.²² This system has been chosen because the analysis of the specific heat suggests a noncollinear amplitude modulated magnetic structure.²⁰ Powder diffraction patterns taken at 25 and 3 K are shown in Fig. 2 (for each pattern the background signal has been subtracted). The pattern at 25 K in the magnetically disordered state can be indexed according to the tetragonal ThCr₂Si₂ structure with $a = 0.4245$ nm and $c = 1.0165$ nm. At 3 K the magnetic lines (for $Q < 2 \text{ \AA}^{-1}$) can be indexed with the propagation vector $\boldsymbol{\tau} = (1/2 \ 0 \ 1/2)$.

The propagation vector and the orientation of the magnetic moments have been varied and the calculated diffraction patterns have been compared to the experimental data. Modules of the *McPhase* software²³ have been used for these computations. The absorption has been calculated for our experimental geometry according to the method given in Ref. 24. It was found to be of minor importance compared to the Lorentz factor in the low angle range, where the magnetic intensities have been refined. For the calculation of the intensity profile a Gaussian lineshape with an angle dependent linewidth was applied. Due to the limited resolution the fit is not very sensitive to small changes of the propagation

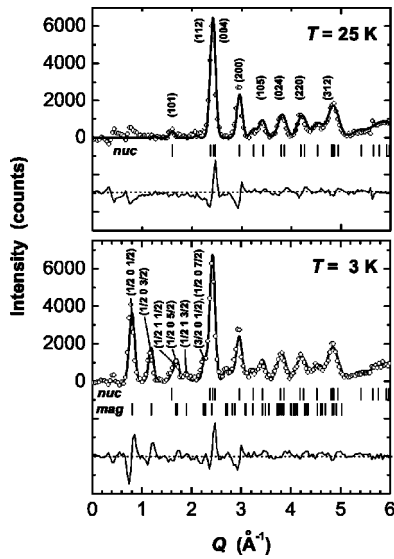


FIG. 2. Neutron diffraction patterns of GdAu_2Si_2 at $T=25$ and 3 K. The lines correspond to the calculated pattern; below each pattern the difference between the calculated and measured intensities is shown. The positions of nuclear peaks and the magnetic satellites with strong intensity are indicated by the vertical bars.

vector. However, the magnetic intensities are very sensitive to the orientation of the magnetic moments.

The best fit of the intensities could be achieved with moments of $6.2\mu_B$ oriented parallel to $[0\ 1\ 0]$, i.e., transversal to the propagation vector $\tau=(1/2\ 0\ 1/2)$. The magnetic unit cell is shown in Fig. 3. Due to the tetragonal symmetry there exist two domains.

Note that the propagation $\tau=(1/2\ 0\ 1/2)$ must lead to an equal moment structure and is not compatible with the non-collinear amplitude modulated structure indicated by the specific heat.²⁰ Consequently either the propagation at temperatures near T_N must differ from $(1/2\ 0\ 1/2)$ or critical fluctuations should be taken into account in more detail to improve the interpretation of the specific heat in this system.

The dipolar model was applied to GdAu_2Si_2 in order to investigate the influence of the dipole interaction. The Fourier transform $\mathcal{J}_{\alpha\beta}(\tau)$ was calculated by applying Eqs. (1)–(3) to the case of GdAu_2Si_2 as shown in Fig. 1. The largest

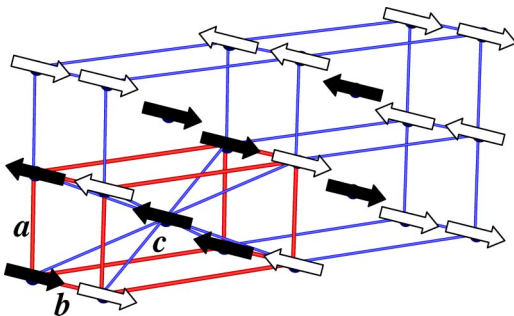


FIG. 3. Magnetic unit cell of GdAu_2Si_2 (domain with $\tau=(1/2\ 0\ 1/2)$ and magnetic moments parallel to $[0\ 1\ 0]$). For clarity we show only the Gd sublattice. The full arrows indicate the primitive basis of the magnetic structure.

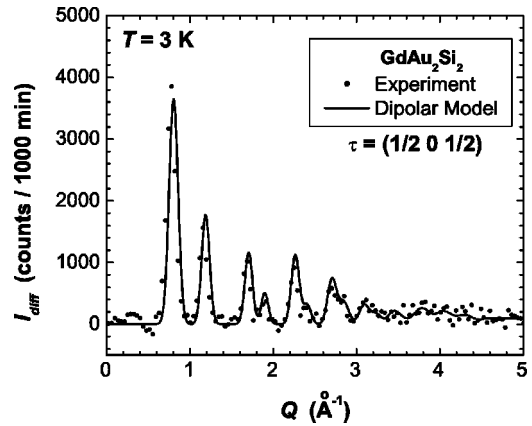


FIG. 4. Magnetic neutron diffraction pattern (data points) of GdAu_2Si_2 as determined from the difference of measurements at $T=4$ and 25 K. The lines correspond to the pattern calculated from the dipolar model described in the text.

eigenvalue corresponds to the moment direction $[0\ 1\ 0]$. This is in agreement with the results of the diffraction experiment and indicates that the dipole interaction is the dominant source of anisotropy in this system. The experimental magnetic diffraction pattern and the pattern calculated from the dipolar model are compared in Fig. 4. For the other compounds of this study a similar analysis has been performed.

B. GdCu_2In

GdCu_2In crystallizes in the cubic Heusler structure $L2_1$ (Ref. 25) (lattice constant $a=0.662$ nm at 2 K). It orders antiferromagnetically below $T_N\sim 10$ K with some complicated and up to now unknown magnetic structure.^{26,27} Thermal expansion was measured²⁷ on polycrystalline samples using a capacitance dilatometer. The estimated value of the magneto-volume effect at 0 K is small ($(\Delta V/V)_{mag}\approx -1\times 10^{-4}$).

We investigated the magnetic structure of the Heusler compound GdCu_2In by neutron diffraction and found complex antiferromagnetism. The propagation vector and the orientation of the magnetic moments have been varied and the calculated magnetic diffraction patterns have been compared to the experimental data taken at $T=2$ K. Figure 5 shows the difference pattern of measurements at 20 and 2 K. The best fit could be achieved with a propagation of $\tau=(1/3\ 1\ 0)$ and a moment direction perpendicular to $[001]$.

The dipolar model for this propagation predicts a collinear amplitude modulated magnetic structure with moments parallel to $[100]$. This moment direction is consistent with the experimental result. However, the quantitative agreement of the powder pattern of this calculated magnetic structure with the experiment is not completely satisfying (see the thin lines in Fig. 5). The reason for this discrepancy is a slight modification of the magnetic structure at lower temperatures which cannot be modeled because the calculation procedure outlined in Sec. II is strictly valid only for temperatures near T_N .

In order to remove this restriction of the model a large effort was undertaken to extend the theoretical analysis to

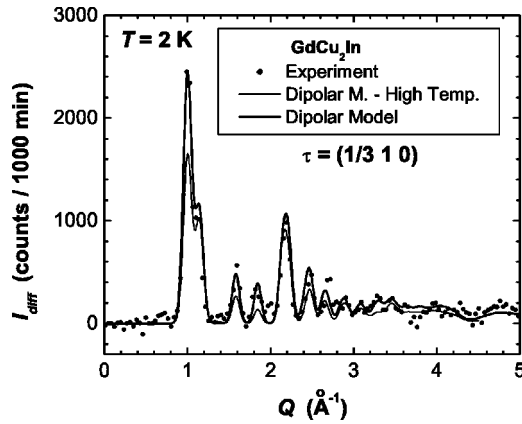


FIG. 5. Magnetic neutron diffraction pattern (data points) of GdCu_2In as determined from the difference of measurements at $T=2$ and 20 K. The lines correspond to the pattern calculated from the dipolar model described in the text. Extending the temperature range of the model (the high temperature expansion is shown by a thin line) to low temperatures by numerical methods (thick line) improves the description of the experimental data (see the text).

low temperatures by numerical methods.²⁸ In a first step *isotropic* short range exchange interaction constants have been set up such as to give a maximum of the Fourier transform at $(1/3 \ 1 \ 0)$ and to reflect the experimental Néel temperature (for details on this procedure see Ref. 9). From these conditions equations for the isotropic exchange parameters follow which can be fulfilled only if more than three neighbors are considered. Therefore, in the model calculation we used the following four nearest neighbor interaction constants, which are associated with the neighbors at $(1/2 \ 1/2 \ 0)$ (-0.0333 meV), $(1 \ 0 \ 0)$ (0.012 meV), $(1/2 \ 1/2 \ 1)$ (0.004 meV), and $(2 \ 0 \ 0)$ (-0.002 meV). In addition to these short range isotropic exchange constants the dipolar interaction as given by equ. (3) was taken into account for distances up to 4 nm. The program *McPhase* (Refs. 23 and 43) was used to calculate the temperature dependence of the magnetic structure. At low temperature a noncollinear magnetic structure is predicted by the calculation. When increasing the temperature to $0.9T_N$ a spin reorientation associated with a change of the magnetic structure from noncollinear to collinear (with moments parallel to $[010]$ in agreement with the analytical approach–II. Dipolar Model) has been computed.

The experimental magnetic diffraction pattern of GdCu_2In at 2 K is in good agreement with the predictions by the model based on isotropic short range exchange plus classical dipolar interactions (see Fig. 5, thick line). Note that a magnetic moment of $6.0 \mu_B/\text{Gd}$ has been used in the calculation.

C. GdAg_2 and GdAu_2

GdAg_2 and GdAu_2 crystallize in the tetragonal MoSi_2 -type structure.²⁹ The space group is $I4/mmm$ with Gd on the 2a sites (point symmetry $4/mmm$) and Ag(Au) on the $4e$ sites. This structure can roughly be viewed as being composed of three tetragonally distorted body centered cubes along c -direction (GdAg_2 : $a=0.3716$ nm, $c=0.926$ nm; GdAu_2 : $a=0.3716$ nm, $c=0.8996$ nm). The z atomic posi-

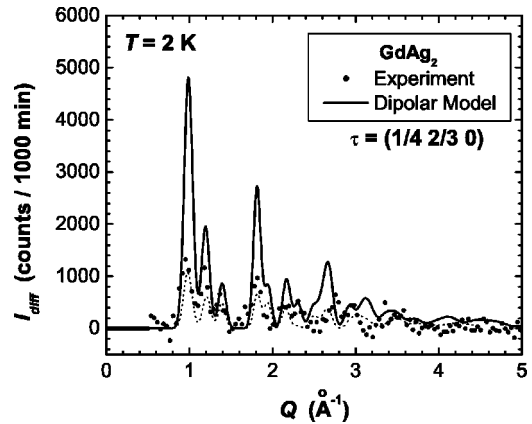


FIG. 6. Magnetic neutron diffraction pattern (data points) of GdAg_2 as determined from the difference of measurements at $T=2$ and 35 K. The straight line corresponds to the pattern calculated from the dipolar model described in the text. The dotted line corresponds to Rietveld type fits, which have been used to determine the magnetic propagation vector.

tion parameter of the $4e$ sites (point symmetry $4mm$) is about $1/3$. For GdAg_2 a value of $z_{Ag} = 0.327 \pm 0.004$ has been determined from neutron diffraction experiments.³⁰

GdAg_2 has first been reported to order magnetically at about 27 K from resistivity measurements.³¹ Further studies^{30,32} including specific heat, resistivity, thermal expansion and magnetization measurements as well as first neutron powder diffraction experiments, showed that this compound orders antiferromagnetically below $T_N \approx 23$ K with two further first-order magnetic transitions at $T_{R1} \approx 21$ K and $T_{R2} \approx 11$ K. The observed first-order magnetic transitions in the ordered range have been attributed to anisotropic terms in the two-ion Gd-Gd exchange interaction. A further peculiarity is that the magnetic ordering temperature of GdAg_2 is lower than in TbAg_2 ($T_N \approx 35$ K), violating the de Gennes law. Recently, the role of biquadratic exchange for the magnetic

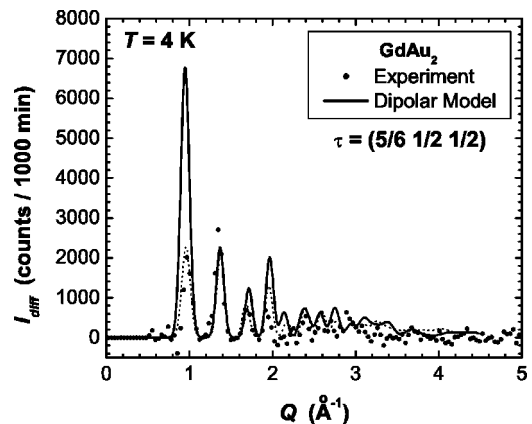


FIG. 7. Magnetic neutron diffraction pattern (data points) of GdAu_2 as determined from the difference of measurements at $T=4$ and 70 K. The straight line corresponds to the pattern calculated from the dipolar model described in the text. The dotted line corresponds to Rietveld type fits, which have been used to determine the magnetic propagation vector.

TABLE I. Magnetic anisotropies of several Gd compounds in comparison with the prediction from the dipole interaction. The second column describes the experimental method (n-neutron diffraction, x-magnetic X-ray scattering, m-Moessbauer spectroscopy, μ SR-muon spin relaxation). In the third column the ordering temperatures are given. The fourth column contains the propagation vector, and the fifth the experimentally derived moment direction at low temperature (moment direction coordinates $[m_x, m_y, m_z]$ refer to Euclidean coordinate system with $x||a$, $y||b$ and $z||c$). In many cases the experimental data are in agreement with the prediction from the dipole interaction given in column six, exceptions are GdAg₂ and GdAu₂. The last column contains the differences Δ_1 and Δ_2 of the eigenvalues of $\mathcal{J}_{\alpha\beta}(\boldsymbol{\tau})$, which are a measure of the dipolar anisotropy. The corresponding eigenvectors are given in brackets (compare Fig. 1).

Experiment			Theory			
Compound	Method	Ordering temperature (K)	Propagation vector $\boldsymbol{\tau}$	Experimental moment direction	Calculated moment direction	Dipolar anisotropy $\Delta_1^{[e_1]} \Delta_2^{[e_2]}$ (μ eV)
cubic						
GdAg (bcc)	n (Ref. 34)	134	(1/2 1/2 0)	[0 0 1]	[0 0 1]	36 ^[100] 36 ^[010]
GdCu (bcc)	n (Ref. 35)	150	(1/2 1/2 0)	[0 0 1]	[0 0 1]	41 ^[100] 41 ^[010]
GdX (fcc, X = S, P, Se)	n (Refs. 36 and 37)	50, 28, 60	(3/2 3/2 3/2)	\perp [1 1 1]	\perp [1 1 1]	0 53, 50, 48 ^[111]
(X = As, Sb, Bi)	n (Refs. 36 and 37)	15.2, 32, 19	(3/2 3/2 3/2)	\perp [1 1 1]	\perp [1 1 1]	0 47, 39, 37 ^[111]
GdCu ₂ In	n (this work)	10	(1/3 1 0)	\perp [0 0 1]	[1 0 0] ^a	2.9 ^[001] 12.3 ^[010]
GdCu ₄ In	n (Ref. 38)	7	(0 1/2 1)	[0 1 0]	[0 1 0]	4.9 ^[100] 4.9 ^[001]
hexagonal						
GdNi ₅	μ SR (Ref. 18)	32	(0 0 0)	[0 0 1]	[0 0 1]	7.5 ^[100] 7.5 ^[010]
GdCuSn ^b	m (Ref. 39)	24	(0 1/2 0)	[0 0 1]	[0 0 1]	12 ^[100] 50 ^[010]
tetragonal						
GdAg ₂	n (this work)	22.7	(1/4 2/3 0)	[1 1 0]	[0.98 0.20 0] ^c	4.3 ^[001] 12.3 ^[-0.20 0.98 0]
GdAu ₂	n (this work)	50	(5/6 1/2 1/2)	\perp [0 1 1]	[1 0 0] ^d	7 ^[0 0.20 0.98] 35 ^[0 0.98 -0.20]
GdAu ₂ Si ₂	n (this work)	12	(1/2 0 1/2)	[0 1 0]	[0 1 0]	11 ^[-0.22 0 0.97] 32 ^[0.97 0 0.22]
GdCu ₂ Si ₂	n (Ref. 40)	12.5	(1/2 0 1/2)	[0 1 0]	[0 1 0]	13 ^[-0.2 0 0.98] 38 ^[0.98 0 0.2]
GdNi ₂ Si ₂	n (Ref. 40)	14.5	(0.207 0 0.903)	[0 1 0]	[0 1 0]	14 ^[-0.99 0 0.13] 34 ^[0.13 0 0.99]
GdNi ₂ B ₂ C	n, x (Ref. 41)	20	(0.55 0 0)	[0 1 0]	[0 1 0]	21 ^[001] 50 ^[100]
orthorhombic						
GdBa ₂ Cu ₃ O ₇	n (Ref. 42)	2.2	(1/2 1/2 1/2)	[0 0 1]	[0 0 1]	14 ^[010] 15 ^[100]

^aNote: extending the theory to $T \rightarrow 0$ by a *McPhase* calculation gives a noncollinear equal moment structure with moments \perp [0 0 1] in agreement with the experiment.

^bNote: only the Gd sublattice has one Gd atom per unit cell. The full structure has two Gd atoms per primitive unit cell.

^cNote: extending the theory to $T \rightarrow 0$ by a *McPhase* calculation gives a noncollinear equal moment structure with moments \perp [0 1 0].

^dNote: extending the theory to $T \rightarrow 0$ by a *McPhase* calculation gives a noncollinear equal moment structure with moments \perp [0, 0.98, -0.2].

properties of these ($L=0$) compounds has been pointed out.⁵ This has been referred to as a change in the conduction band due to the boundary situation of GdAg₂ concerning the crystal structure, i.e., only the RAg₂ compounds with heavy rare earth, starting from Gd, show the MoSi₂ type of structure.³⁰

In the previous neutron diffraction experiments by Gignoux *et al.*³⁰ magnetic satellites have been found below the ordering temperature. However, the data has to be doubted, because at the position of the (002) nuclear reflection no intensity has been found at any temperature in contrast to expectations from the reported crystallographic structure. Therefore, the magnetic scattering at low angles also has to be doubted, and we decided to remeasure GdAg₂.

Indeed our new data are in excellent agreement with the reported crystallographic structure, including the intensity on the (002) nuclear reflection. Figure 6 shows the magnetic diffraction pattern as determined from the difference of mea-

surements at 2 and 35 K. Fitting suggests a propagation of $\boldsymbol{\tau} = (1/4 \ 2/3 \ 0)$ (dotted lines). The best fit of the 2-K pattern with this propagation corresponds to an amplitude modulated structure with moments in the [110] direction. The prediction of classical dipolar exchange (just below the ordering temperature) is a moment direction along [0.98, 0.20, 0], which is more or less along *a* direction.

In order to make a correct theoretical prediction of the squaring up at temperatures far below T_N a *McPhase* calculation has been performed similar to the case of GdCu₂In. At 2 K a cycloid in the *ac* plane is predicted. However, the magnetic pattern calculated in this way is in clear disagreement with the experimental pattern (see Fig. 6, straight line).

GdAu₂ orders antiferromagnetically like GdAg₂, but at a much higher ordering temperature of $T_N \approx 50$ K.³³ In contrast to GdAg₂ there is no measurable spontaneous magneto-elastic effect at all. The magnetically induced change of *c/a*

as well as the volume magnetostriction of GdAu_2 is smaller than 10^{-4} .³² The results of our neutron diffraction study for determining the magnetic structure are shown in Fig. 7. The best fit gives a propagation of $\tau=(5/6 \ 1/2 \ 1/2)$ with an equal moment cycloid with moments perpendicular to $[011]$.

However, the classical dipolar interaction predicts collinear moments parallel to $[100]$ for this propagation (near the ordering temperature). At lower temperatures a *McPhase* calculation gives an equal moment cycloid with moments perpendicular to $[0,0.98,-0.2]$. The predicted intensities do not correspond to the experimental data.

Provided that the propagation vectors are correct (small deviations from the assumed propagation vectors will not alter the result) the experimental data indicates, that in GdAg_2 and GdAu_2 the classical dipolar model for the anisotropy of the two ion interactions cannot describe the experimental moment direction sufficiently. Note that in both cases the dipolar anisotropy is rather small (see Table I), and therefore other sources of anisotropy may become important.

IV. DISCUSSION

For generalization we now consider other available data for compounds with one Gd atom per primitive crystallographic unit cell. Table I shows a list of the compounds which have been investigated and which we have subjected to our model analysis. Most of the experimental data have been derived from neutron diffraction. The moment directions taken from the experiment are compared to the calculation and agree for almost all cases under investigation.

In order to give a measure of the dipolar anisotropy for every compound the differences Δ_1 and Δ_2 of eigenvalues of $\mathcal{J}_{\alpha\beta}(\tau)$ (compare Fig. 1) are given in the last column of Table I. For orientation the eigenvectors \mathbf{e}_1 and \mathbf{e}_2 are also listed, which correspond to the hard moment directions. The

values of Δ_1 and Δ_2 show, that the dipolar anisotropy varies over one order of magnitude. It is largest for the 1:1 compounds (short Gd-Gd distances) and smallest for GdNi_5 . It is small also in those few cases where the dipolar model fails (GdAg_2 and GdAu_2). Note that *cubic ferromagnets* such as GdMg (Ref. 5) have not been listed, because in this case the dipolar anisotropy is zero by symmetry. To our knowledge no experimental determination of the moment direction (easy axis) has been reported in this very interesting class of compounds.

In conclusion, in this paper we have shown that in many Gd compounds the observed anisotropy originates from the dipole interaction. Thus the compounds under consideration might behave according to the dipolar universality class as described in Refs. 15 and 16 for the case of Gd metal. Although the magnetic anisotropy of Gd compounds is usually much smaller than that of the other rare earth compounds, it can be predicted with a much higher accuracy from first principles. However, care must be taken if the dipolar anisotropy energy Δ_1 (as defined in our model-section II) is less than $10 \mu\text{eV}$. Then other sources of anisotropy become important, which still have to be identified for the compounds under consideration.

ACKNOWLEDGMENTS

We are grateful to the valuable comments of U. Köbler and P. Maier on the paper and J. P. Ambroise for helpful assistance at LLB, Saclay. Part of this work was performed within the program of the Sonderforschungsbereich 463 (funded by the Deutsche Forschungsgemeinschaft). We acknowledge financial support by the Austrian Science Fund (FWF) Project No. P-14932-PHY, by the Austrian Academy of Sciences (APART 10739) and by the European Commission in the frame of the HPRI access program.

*Electronic address: rotter@physik.tu-dresden.de

¹K.W.H. Stevens, *Magnetic Ions in Crystals* (Princeton University Press, Princeton, 1997).

²J. Jensen and A.R. Mackintosh, *Rare Earth Magnetism* (Clarendon Press, Oxford, 1991).

³F. Simon, A. Rockenbauer, T. Feher, A. Janossy, C. Chen, A.J.S. Chowdhury, and J.W. Hodby, *Phys. Rev. B* **59**, 12072 (1999).

⁴R.W. Cochrane, C.Y. Wu, and W.P. Wolf, *Phys. Rev. B* **8**, 4348 (1973).

⁵U. Köbler, R.M. Müller, P.J. Brown, and K. Fischer, *J. Phys.: Condens. Matter* **13**, 6835 (2001).

⁶W.P. Wolf, *J. Phys. (Paris), Colloq.* **32**, C-1 (1971).

⁷A. Loidl, K. Knorr, J.K. Kjems, and B. Luethi, *Z. Phys. B: Condens. Matter* **35**, 253 (1979).

⁸B. Halg and A. Furrer, *Phys. Rev. B* **34**, 6258 (1986).

⁹M. Rotter, M. Loewenhaupt, S. Kramp, T. Reif, N.M. Pyka, W. Schmidt, and R.v.d. Kamp, *Eur. Phys. J. B* **14**, 29 (2000).

¹⁰M. Rotter *et al.* *Phys. Rev. B* **64**, 134405 (2001).

¹¹N.M. Fujiki, K. De'Bell, and D.J.W. Geldart, *Phys. Rev. B* **36**, 8512 (1987).

¹²D.J.W. Geldart, P. Hargraves, N.M. Fujiki, and R.A. Dunlap, *Phys. Rev. Lett.* **62**, 2728 (1989).

¹³J.M. Coey, V. Skumryev, and K. Gallagher, *Nature (London)* **401**, 35 (1999).

¹⁴S.N. Kaul and S. Srinath, *Phys. Rev. B* **62**, 1114 (2000).

¹⁵S. Henneberger, E. Frey, P.G. Maier, F. Schwabl, and G.M. Kalvius, *Phys. Rev. B* **60**, 9630 (1999).

¹⁶S. Srinath and S.N. Kaul, *Phys. Rev. B* **60**, 12 166 (1999).

¹⁷M. Colarieti-Tosti, S.I. Simak, R. Ahuja, L. Nordström, O. Eriksson, and M.S.S. Brooks, *J. Magn. Magn. Mater.* (in press).

¹⁸A. Yaouanc, P. Dalmas de Réotier, P.C.M. Gubbens, A.M. Mulders, F.E. Kayzel, and J.J.M. Franse, *Phys. Rev. B* **53**, 350 (1996).

¹⁹M.T. Hutchings, R.J. Birgeneau, and W.P. Wolf, *Phys. Rev.* **168**, 1026 (1968).

²⁰M. Rotter, M. Loewenhaupt, M. Doerr, A. Lindbaum, and H. Michor, *Phys. Rev. B* **64**, 014402 (2001).

²¹A. Aharony and M.E. Fisher, *Phys. Rev. B* **8**, 3323 (1973).

²²R. Mallik and E.V. Sampathkumaran, *Phys. Rev. B* **58**, 9178 (1998).

²³M. Rotter, *J. Magn. Magn. Mater.* (in press).

²⁴D. Schmitt and B. Ouladdiaf, *J. Appl. Crystallogr.* **31**, 620 (1998).

²⁵P.J. Webster, *Contemp. Phys.* **10**, 559 (1969).

²⁶M.J. Parsons, J. Crangle, K.U. Neumann, and K.R.A. Ziebeck, *J.*

- Magn. Magn. Mater. **184**, 184 (1998).
- ²⁷J.W. Taylor, H. Capellmann, K.U. Neumann, and K.R.A. Ziebeck, Eur. Phys. J. B **16**, 233 (2000).
- ²⁸M. Rotter, M. Doerr, M. Loewenhaupt, A. Lindbaum, K. Ziebeck, and B. Beuneu, Physica B (in press).
- ²⁹A. Dwight, J. Downey, and R. Conner, Acta Crystallogr. **22**, 745 (1967).
- ³⁰D. Gignoux, P. Morin, and D. Schmitt, J. Magn. Magn. Mater. **102**, 33 (1991).
- ³¹M. Ohashi, T. Kaneko, and S. Miura, J. Phys. Soc. Jpn. **38**, 588 (1975).
- ³²A. Lindbaum and M. Rotter, in *Magnetic Materials*, edited by K.H.J. Buschow (Elsevier, Amsterdam, 2002), Vol. 14, pp. 307–362.
- ³³L.D. Tung, K.H.J. Buschow, J.J.M. Franse, and N.P. Thuy, J. Magn. Magn. Mater. **154**, 96 (1996).
- ³⁴T. Chattopadhyay, G.J. McIntyre, and U. Köbler, Solid State Commun. **100**, 117 (1996).
- ³⁵J.A. Blanco, J.I. Espeso, J.I. García Soldevilla, J.C. Gómez Sal, M.R. Ibarra, C. Marquina, and H.E. Fischer, Phys. Rev. B **59**, 512 (1999).
- ³⁶T.R. McGuire, R.J. Gambino, S.J. Pickart, and H.A. Alperin, J. Appl. Phys. **40**, 1009 (1969).
- ³⁷F. Hulliger, J. Magn. Magn. Mater. **8**, 183 (1978).
- ³⁸H. Nakamura, N. Kim, M. Shiga, R. Kmieć, K. Tomala, E. Ressouche, J.P. Sanchez, and B. Malaman, J. Phys.: Condens. Matter **11**, 1095 (1999).
- ³⁹D. Bialic, R. Kruk, R. Kmieć, and K. Tomala, J. Alloys Compd. **257**, 49 (1997).
- ⁴⁰J.M. Barandiaran, D. Gignoux, D. Schmitt, J.C. Gomez-Sal, J.R. Fernandez, P. Chieux, and J. Schweizer, J. Magn. Magn. Mater. **73**, 233 (1988).
- ⁴¹C. Detlefs, A.I. Goldman, C. Stassis, P.C. Canfield, B.K. Cho, J.P. Hill, and D. Gibbs, Phys. Rev. B **53**, 6355 (1996).
- ⁴²D.M. Paul, H.A. Mook, A.W. Hewat, B.C. Sales, L.A. Boatner, J.R. Thompson, and M. Mostoller, Phys. Rev. B **37**, 2341 (1988).
- ⁴³www.mcphase.de